

BOUNDARY PARAMETRIZATION OF PLANAR SELF-AFFINE TILES WITH COLLINEAR DIGIT SET

SHIGEKI AKIYAMA AND BENOÎT LORIDANT

ABSTRACT. We consider a class of planar self-affine tiles T generated by an expanding integral matrix \mathbf{M} and a collinear digit set \mathcal{D} as follows :

$$\mathbf{M} = \begin{pmatrix} 0 & -B \\ 1 & -A \end{pmatrix}, \mathcal{D} = \left\{ \begin{pmatrix} 0 \\ 0 \end{pmatrix}, \dots, \begin{pmatrix} |B| - 1 \\ 0 \end{pmatrix} \right\}.$$

We give a parametrization $\mathbb{S}^1 \rightarrow \partial T$ of the boundary of T with standard properties. It is Hölder continuous and associated to a sequence of simple closed polygonal approximations whose vertices lie on ∂T and have algebraic preimages. We derive a new proof that T is homeomorphic to a disk if and only if $2|A| \leq |B + 2|$.

1. INTRODUCTION

Self-affine tilings in \mathbb{R}^d have attracted wide attention in modeling self-similar structures which appear in many branches of mathematics. It is believed that the boundary of self-affine tiles has non-integral dimension unless the tile is polygonal [20, 21]. Indeed the boundary of self-affine tiles often shows a fractal shape, and its topological study is rather difficult.

In [1], we introduced a standard method to parametrize the boundary of self-affine tiles if the associated contact automaton is strongly connected. More precisely we expect that whenever the tile is connected, there exists an oriented extension of the contact automaton which parametrizes the boundary. And this parametrization is Hölder continuous and precisely described by a cyclic version of Dumont-Thomas number system. We confirmed the existence of such oriented automata for tiles associated to quadratic canonical number systems.

In this paper, we wish to continue this study of parametrization in the case that the contact automaton is not strongly connected. For this purpose, we study a wider class of tiles corresponding to 2×2 integral expanding matrix $\mathbf{M} = \begin{pmatrix} 0 & -B \\ 1 & -A \end{pmatrix}$ with collinear digits sets. There are two new aspects to be taken into account in this class. Firstly, the multiplication of the expanding matrix may involve *flipping*, *i.e.*, the direction of the boundary pieces may change. To get a parametrization in this case, we introduce a certain duplicated automaton whose states keep information on alternating direction. Second is that the contact automaton is no longer strongly connected, but has two strongly connected components. Thus we have to introduce two independent parameterizations and merge them into one. Nevertheless, we can derive exactly the same standard properties of the parametrization, *i.e.*, it gives step by step approximation of the boundary by polygonal curves which are topological circles, whose vertices are the fixed point of the GIFS and have natural algebraic addresses. Further it intertwines Lebesgue measure on the unit circle to a certain Hausdorff measure which is positive and finite on the boundary of the tile.

To simplify the study, we introduce a noteworthy correspondence between tiles corresponding to A and $-A$ which basically comes from the symmetry of digits. This somewhat halves our effort for topological classification of planar tiles with collinear digits and we reprove the result of Leung-Lau [16] that the tiles are disk-like if and only if $2|A| \leq |B + 2|$.

Date: September 24, 2014.

The authors are supported by Japanese Ministry of Education, Culture, Sports, Science and Technology, Grant-in Aid for fundamental research 21540010 and the Japanese Society for the Promotion of Science, grant 08F08714.

2. STATEMENT OF THE MAIN RESULTS

Let \mathbf{M} be a $d \times d$ integral *expanding* matrix, *i.e.*, with eigenvalues greater than 1 in modulus, and $\mathcal{D} \subset \mathbb{Z}^d$ a finite set. Then there is a unique nonempty compact set $T = T(\mathbf{M}, \mathcal{D})$ satisfying

$$\mathbf{M}T = \bigcup_{a \in \mathcal{D}} (T + a) \quad (2.1)$$

(see [10]). Suppose that $\mathcal{D} \subset \mathbb{Z}^d$ is a complete residue system of $\mathbb{Z}^d/\mathbf{M}\mathbb{Z}^d$. Then T has positive Lebesgue measure (see [14]) and we call it *integral self-affine tile with digit set \mathcal{D}* . It is known [15] that there is a sublattice \mathcal{J} of \mathbb{Z}^d such that $T + \mathcal{J}$ is a *tiling of \mathbb{R}^d* :

$$\bigcup_{s \in \mathcal{J}} (T + s) = \mathbb{R}^d \quad \text{and} \quad \lambda_d((T + s) \cap (T + s')) = 0 \text{ if } s \neq s' \in \mathcal{J},$$

where λ_d is the d -dimensional Lebesgue measure. If $\mathcal{J} = \mathbb{Z}^d$, we call T a self-affine \mathbb{Z}^d -tile.

In the plane, a basic question is the *disk-likeness* of the central tile T , that is, the homeomorphy to a closed disk. In [3], a criterion was given in terms of number and configuration of the neighbors of T in the induced tiling. The case of a collinear digit set was then completely characterized in [16]. Suppose that \mathbf{M} has the characteristic polynomial $x^2 + Ax + B$ and $\mathcal{D} = \{0, v, 2v, \dots, (|B| - 1)v\}$ for some $v \in \mathbb{Z}^2$ such that $v, \mathbf{M}v$ are linearly independent. Then T is disk-like if and only if $2|A| \leq |B + 2|$. The proof relies on the criterion mentioned above and an analysis of the triple points of the tiling. This generalized a result of [2] for quadratic canonical number system tiles. The usual technique consists in showing that the interior of T is connected.

Recently the authors proposed in [1] a standard method to parametrize the boundary of a self-affine \mathbb{Z}^d -tile $T(\mathbf{M}, \mathcal{D})$. As a consequence, disk-likeness of the tile is obtained directly by showing that its boundary is a simple closed curve. In the present paper, we wish to illustrate this method and reprove the above result of Leung-Lau (see Proposition 5.2). Without loss of generality, we may deal with the following class of self-affine \mathbb{Z}^2 -tiles:

$$\mathbf{M} = \begin{pmatrix} 0 & -B \\ 1 & -A \end{pmatrix}, \quad \mathcal{D} = \left\{ \begin{pmatrix} 0 \\ 0 \end{pmatrix}, \dots, \begin{pmatrix} |B| - 1 \\ 0 \end{pmatrix} \right\}. \quad (2.2)$$

Indeed, let $(\mathbf{M}_0, \mathcal{D}_0)$ as in the previous paragraph: \mathbf{M}_0 has characteristic polynomial $x^2 + Ax + B$ and $\mathcal{D}_0 = \{0, v, 2v, \dots, (|B| - 1)v\}$ is such that v, \mathbf{M}_0v are linearly independent. Denote by \mathbf{C} the matrix of change of basis from the canonical basis to (v, \mathbf{M}_0v) . Then the relations

$$\mathbf{M} = \mathbf{C}^{-1}\mathbf{M}_0\mathbf{C}, \quad \mathcal{D} = \mathbf{C}\mathcal{D}_0$$

hold. It follows that $T(\mathbf{M}_0, \mathcal{D}_0) = \mathbf{C}T(\mathbf{M}, \mathcal{D})$. Therefore, we will restrict ourselves to the subclass (2.2), whose topological properties can be transferred to the whole class treated in [16]. Note that \mathbf{M} is expansive iff $|A| \leq B$ if $B \geq 2$, or $|A| \leq |B + 2|$ if $B \leq -2$. The tiles corresponding to $A = 2, B = -6$ (disk-like) and $A = 1, B = -3$ (non disk-like) are depicted in Figure 1. Note that for $A = 0$, the tile is just a rectangle. Thus we will suppose $A \neq 0$.

Part of this class was already studied as example in [1], namely for $0 < A \leq B \geq 2$. The case $B \geq 2, A < 0$ can be treated similarly. However, for $B \leq -2$, two new phenomena occur as explained below.

The main tool to parametrize ∂T is the *reduced contact automaton* $G(\mathcal{R})$. It is deduced from the contact automaton that was introduced in [8] to compute the fractal dimension of ∂T . We will recall its construction in Section 3. It has a finite and symmetric set of states $\mathcal{R} = -\mathcal{R}$ and transitions labeled by elements of \mathcal{D} . It gives a description of the boundary of T as the attractor of a *graph iterated function system*, or *GIFS* for short:

$$\partial T = \bigcup_{s \in \mathcal{R}} K_s \quad (2.3)$$



FIGURE 1. Tiles with collinear digit set : $A = 2, B = -6$ (left) and $A = 1, B = -3$ (right).

and

$$K_s = \bigcup_{s \xrightarrow{a} s' \in G(\mathcal{R})} \mathbf{M}^{-1}(K_{s'} + a) \quad (2.4)$$

for a (unique) vector $(K_s)_{s \in \mathcal{R}}$ of non-empty compact sets. By [1], if the automaton $G(\mathcal{R})$ is strongly connected and some compatibility conditions are satisfied, then the parametrization can be performed. The method is valid for our class in the case $B \geq 2$. We will show how to adapt it for the case $B \leq -2$.

The first new phenomenon is the following. For $\det(\mathbf{M}) = B < 0$, one observes a flipping of the boundary pieces. That is, the orientation of the boundary pieces changes at each iteration of (2.4) (see Figure 3). Of course, one may think of taking \mathbf{M}^2 instead of \mathbf{M} . This would keep the number of states of $G(\mathcal{R})$ but would have the disadvantage to square the number of digits. Indeed, \mathcal{D} should be replaced by $\mathcal{D} + \mathbf{M}\mathcal{D}$. We will rather fake the flipping by doubling the number of states.

- For each state $S \in \mathcal{R}$, we create the states S and \bar{S} .
- For each transition $S \xrightarrow{a} T \in G(\mathcal{R})$, we create the transitions $S \xrightarrow{a} \bar{T}$ and $\bar{S} \xrightarrow{a} T$.

The resulting automaton is denoted by $G'(\mathcal{R})$. It has $2 \times |\mathcal{R}|$ states. It is also a GIFS for the boundary, but each boundary part K_s has been duplicated (compare Figure 2 and Figure 4). This will allow us to switch between two different orientations of a same boundary part.

We denote by G the automaton $G(\mathcal{R})$ if $B > 0$ or $G'(\mathcal{R})$ if $B < 0$. We write r for the number of states of G : $r = |\mathcal{R}|$ or $r = 2|\mathcal{R}|$. Let us order arbitrarily the set of vertices and the transitions of G . Thus (2.3) and (2.4) now read

$$\partial T = \bigcup_{i=1}^r K_i, \quad K_i = \bigcup_{i \xrightarrow{a|\mathbf{o}} j} \mathbf{M}^{-1}(K_j + a). \quad (2.5)$$

Here, the transitions starting from i have been ordered (label \mathbf{o}) from 1 and l_{max}^i , the number of these transitions. We call G^O this *ordered extension*. It gives rise to a mapping

$$\begin{aligned} \Psi^O : G^O &\rightarrow \partial T \\ w &\mapsto \sum_{j \geq 1} \mathbf{M}^{-j} a_j, \end{aligned} \quad (2.6)$$

for the infinite walk $w = (i; \mathbf{o}_1, \mathbf{o}_2, \dots) := i \xrightarrow{a_1|\mathbf{o}_1} s_1 \xrightarrow{a_2|\mathbf{o}_2} \dots$ of G^O . There are finitely many possible ordered extensions G^O . In Section 3, we will be able to find an ordered extension such that the following *compatibility conditions* are satisfied.

$$\Psi^O(i; \overline{\mathbf{1}_{max}}) = \Psi^O(i+1; \overline{\mathbf{1}}) \quad (1 \leq i \leq r-1) \quad (2.7)$$

$$\Psi^O(r; \overline{\mathbf{1}_{max}}) = \Psi^O(1; \overline{\mathbf{1}}) \quad (2.8)$$

$$\Psi^O(i; \mathbf{o}, \overline{\mathbf{1}_{max}}) = \Psi^O(i; \mathbf{o} + \mathbf{1}, \overline{\mathbf{1}}) \quad (1 \leq i \leq r, 1 \leq o < l_{max}^i). \quad (2.9)$$

Here, $\bar{\mathbf{o}}$ is the infinite repetition $\mathbf{o}\mathbf{o}\dots$. So $(i; \bar{\mathbf{1}})$ is the infinite walk starting from the state i and going along the transitions carrying the minimal order. For simplicity, the notation l_{max} is used without reference to the current state. Therefore, the compatibility conditions express the idea that the boundary parts (K_i) as well as their subdivisions can be ordered “as they appear around the boundary” with matching extremities. In fact, $\partial T = \bigcup_{i=1}^{|\mathcal{R}|} K_i$ also holds in the flipping case $r = 2|\mathcal{R}|$. However, all the walks in the compatibility conditions are wandering along the whole r -states automaton G^O . When $B < 0$, no direct ordering of $G(\mathcal{R})$ can be found to satisfy similar conditions.

We now consider the second new phenomenon. In [1], the connection to the interval $[0, 1]$ is realized via a Dumont-Thomas number system induced by the strongly connected automaton G^O . Here, for $B < 0$, G^O is disconnected. For $A > 0$, $G(\mathcal{R})$ itself is not connected (see Figure 2). For $A < 0$, $G(\mathcal{R})$ is strongly connected but its double sized version fails to be. Nevertheless, in both cases, we shall see that G^O consists of two identical irreducible components. Thus the number system can also be introduced. It runs as follows. Since G^O is made of one ($B > 0$) or two ($B < 0$) copies of $G(\mathcal{R})$, the data for this number system is all contained in $G(\mathcal{R})$. Let $d_{ss'}$ be the number of transitions in $G(\mathcal{R})$ from s' to s . Then the *incidence matrix* is

$$\mathbf{D} := (d_{ss'})_{s, s' \in \mathcal{R}}.$$

Let β be the Perron-Frobenius eigenvalue of \mathbf{D} . A number system in $[0, 1]$ mimics the ordered GIFS (2.5) via uniform subdivisions of the interval $[0, 1]$ (see Section 3). The subdivisions involve power series of $\frac{1}{\beta}$. Identifications occur in the number system. The above compatibility conditions insure that they are reproduced in the boundary of T . This results in a continuous parametrization $C : [0, 1] \rightarrow \partial T$. Whether the parametrization is then injective or not can also be checked. In this case, the tile T is disk-like.

In this way, we will be able to provide a similar description as in [1] for the whole class. Before stating the theorems, we mention that some symmetry relation in our class will reduce the number of cases to be treated. Let

$$\mathbf{P} = \begin{pmatrix} 1 & 0 \\ 0 & -1 \end{pmatrix}, \quad \mathbf{M}_1 = \begin{pmatrix} 0 & -B \\ 1 & -A \end{pmatrix}, \quad \mathbf{M}_2 = \begin{pmatrix} 0 & -B \\ 1 & A \end{pmatrix} \quad (2.10)$$

and \mathcal{D} as in (2.2). Moreover, let $T_1 := T(\mathbf{M}_1, \mathcal{D})$ and $T_2 := T(\mathbf{M}_2, \mathcal{D})$. Then one can check that $\mathbf{P}\mathbf{M}_1\mathbf{P}^{-1} = -\mathbf{M}_2$, $\mathbf{P}\mathcal{D} = \mathcal{D}$ and

$$T_2 = \mathbf{P}T_1 + \underbrace{\sum_{i \geq 0} \mathbf{M}_2^{-2i-1} \begin{pmatrix} |B| - 1 \\ 0 \end{pmatrix}}_{=: \mathbf{v}}. \quad (2.11)$$

This is reflected by a tight connection between the automata describing the boundaries. In the proposition below, we assume the ordered extension to have some symmetry property. It is a natural choice related to symmetries of $G(\mathcal{R})$. The exact definition is given in Section 5.

Proposition 2.1. *For $i = 1, 2$, let T_i as above and G_i the associated reduced contact automata (if $B > 0$) or double sized automata (if $B < 0$). Let G_1^O be any symmetric ordered extension of G_1 . Then there exists an ordered extension G_2^O of G_2 such that the following diagram commutes.*

$$\begin{array}{ccc} G_1^O & \xrightarrow{id} & G_2^O \\ \Psi_1^O \downarrow & & \downarrow \Psi_2^O \\ \partial T_1 & \xrightarrow{f} & \partial T_2 \end{array}$$

Here, $f(x) = \mathbf{P}x + \mathbf{v}$ as in (2.11). Also, id is the identity on the infinite ordered walks $(i; \mathbf{o}_1, \mathbf{o}_2, \dots)$, but the digit labels may not be preserved.

The main theorem reads as follows.

Theorem 1. *Let $(\mathbf{M}, \mathcal{D})$ as in (2.2) and T be the self-similar tile satisfying $\mathbf{M}T = T + \mathcal{D}$. Then there exists an algebraic integer β , a Hölder continuous mapping $C : [0, 1] \rightarrow \partial T$ with $C(0) = C(1)$ and a hexagon Q with the following properties. Let $T_0 := Q$ and $(T_n)_{n \geq 1}$ defined by*

$$\mathbf{M}T_n = T_{n-1} + \mathcal{D}.$$

Then :

- (1) $\lim_{n \rightarrow \infty} \partial T_n = \partial T$ (Hausdorff metric).
- (2) For all $n \in \mathbb{N}$, ∂T_n is a polygonal simple closed curve.
- (3) Denote by V_n the set of vertices of ∂T_n . For all $n \in \mathbb{N}$,

$$V_n \subset V_{n+1} \subset C(\mathbb{Q}(\beta) \cap [0, 1]),$$

i.e., the vertices have $\mathbb{Q}(\beta)$ -addresses in the parametrization.

We can compare the parametrization in the above theorem with a Hausdorff measure on the boundary. Since the tiles are self-affine but not necessarily self-similar, a generalized Hausdorff measure is needed. It relies on a pseudo-norm w for which any expanding affine matrix \mathbf{M} becomes a similarity :

$$w(\mathbf{M}x) = |\det(\mathbf{M})|^{1/2} w(x) \quad (x \in \mathbb{R}^2). \quad (2.12)$$

For this pseudo norm, Hausdorff measures \mathcal{H}_w^α ($\alpha > 0$) and dimensions can be defined in a similar way as for the Euclidean norm (see [9]). The following theorem will be easily derived from [1, Theorem 2], where the contact automaton $G(\mathcal{R})$ was assumed to be strongly connected.

Theorem 2. *Let T as in Theorem 1, C be the corresponding parametrization. Furthermore, let w be a pseudo-norm such that (2.12) holds,*

$$\alpha := 2 \frac{\log(\beta)}{\log(|\det(\mathbf{M})|)}.$$

and \mathcal{H}_w^α the associated Hausdorff measure. Then, for each boundary part K_s ($s \in \mathcal{R}$) as in (2.3),

$$\infty > \mathcal{H}_w^\alpha(K_s) > 0.$$

Moreover, there is a subdivision of the interval $[0, 1]$, $t_0 := 0 < t_1 < \dots < t_{|\mathcal{R}|} := 1$ such that

$$\frac{1}{c} \mathcal{H}_w^\alpha(C([t_i, t_{i+1}])) = t_{i+1} - t_i \quad (t_i \leq t \leq t_{i+1}),$$

where $c := \sum_{s \in \mathcal{R}} \mathcal{H}_w^\alpha(K_s)$.

We compared here subintervals of $[0, 1]$ with the Hausdorff measure on each boundary piece $(K_s)_{s \in \mathcal{R}}$. In order to obtain the measure intertwining map from whole $[0, 1]$ to ∂T , the measure disjointness of these pieces would be needed. This does not follow from the open set condition. This is more related to the Hausdorff dimension of the triple points in the tiling induced by T . In this paper, we do not discuss further this point.

We can link the boundary parametrization to the recurrent set method. This method was introduced by Dekking in [4, 5]. Given an endomorphism

$$\sigma : \langle a, b \rangle \rightarrow \langle a, b \rangle$$

on the free group $\langle a, b \rangle$ generated by two letters and a homomorphism

$$g : \langle a, b \rangle \rightarrow \mathbb{R}^2,$$

the boundary of a self-similar tile is constructed. It is approximated by a sequence of simple closed curves. These curves represent the iterates of σ on the initial word $aba^{-1}b^{-1}$. Under a condition of short range cancellations, the sequence converges in Hausdorff metric to the boundary of a self-similar tile.

In our case, the tile T satisfying $\mathbf{M}T = T + \mathcal{D}$ is given, and we are looking for appropriate boundary substitution σ and embedding g . Let T be a self-affine \mathbb{Z}^2 -tile as in Theorem 1. A substitution arises naturally from the ordered GIFS (2.5). It sends the letter i to the sequence of

letters $j_1 j_2 \dots j_{l_{max}}$ according to the ordered subdivisions in (2.5). We will see that G^O has six ($B > 0$) or twelve ($B < 0$) states. But by reasons of symmetry, the substitution will act on the free group generated by only three letters a, b, c . Furthermore, let Q be the hexagon of Theorem 1. We will prove that $Q + \mathbb{Z}^2$ is a tiling of the plane. We denote by C_1, C_2, \dots, C_6 the consecutive vertices of Q . Then g associates the letters to the sides of ∂Q :

$$g(a) = \mathbf{v}_a := C_2 - C_1, \quad g(b) = \mathbf{v}_b := C_3 - C_2, \quad g(c) = \mathbf{v}_c := C_4 - C_3,$$

and is extended to a homomorphism on $\langle a, b, c \rangle$. Also, given a reduced word $a_1 \dots a_m$, let $p(a_1 \dots a_m)$ stand for the polygonal path joining

$$0, g(a_1), g(a_1 a_2), \dots, g(a_1 \dots a_m)$$

in this order by straight lines. By this correspondence, $p(\sigma(abca^{-1}b^{-1}c^{-1}))$ will be a curve congruent to $\partial(Q + \mathcal{D})$ and more generally, $p(\sigma^n(abca^{-1}b^{-1}c^{-1}))$ a simple closed curve congruent to $\partial(Q + \mathcal{D} + \dots + \mathbf{M}^{n-1}\mathcal{D})$.

Theorem 3. *Let the self-affine tile T and the sequence $(T_n)_{n \geq 0}$ be as in Theorem 1. Then there is an endomorphism $\sigma : \langle a, b, c \rangle \rightarrow \langle a, b, c \rangle$ and a homomorphism $g : \langle a, b, c \rangle \rightarrow \mathbb{R}^2$ with the following properties.*

- (1) For all $n \geq 0$,

$$\underbrace{\mathbf{M}^{-n} p(\sigma^n(abca^{-1}b^{-1}c^{-1}))}_{=: K_n} = \partial T_n + \mathbf{k}_n$$

for some $\mathbf{k}_n \in \mathbb{R}^2$.

- (2) $(K_n)_{n \geq 0}$ converges to a curve K in Hausdorff metric. Moreover,

$$K = \partial T + \mathbf{k}$$

for some $\mathbf{k} \in \mathbb{R}^2$.

The paper is organized as follows. In Sections 3 and 4, we treat the case $A \geq 0$, $B \leq -2$ in details. Indeed, in this case $G(\mathcal{R})$ is disconnected and the flipping occurs. In Section 3, we recall the construction of $G(\mathcal{R})$. We derive the parametrization of ∂T and the associated sequence of approximations. Section 4 is devoted to the recurrent set method. In Section 5, we extend the previous results to the whole class. We prove Proposition 2.1, and our theorems follow. We end up the section with a new proof of the disk-likeness characterization. In Section 6, we eventually make several comments about possible generalizations of our method.

3. $G(\mathcal{R})$ AND THE BOUNDARY PARAMETRIZATION

In this section, we construct the reduced contact automaton $G(\mathcal{R})$. We introduce its ordered extension and obtain the boundary parametrization.

We first recall some definitions on automata. Let Λ be a finite set, or *alphabet*. Its elements are *letters* and sequences of letters are *words*. Λ^* denotes the set of finite words, Λ^ω the set of infinite words. If $l = (l_1, \dots, l_n) \in \Lambda^*$, we write $|l| = n$ for the *length* of l and $l_{|m} = (l_1, \dots, l_m)$ for the *prefix* of l of length $m \leq n$. If $l \in \Lambda^\omega$, then $|l| = \infty$ and prefixes $l_{|m}$ are defined for all $m \geq 1$. The concatenation of two words a and b is denoted by $a \& b$. If a word a is repeated infinitely many times, we write \bar{a} , meaning $a \& a \& a \dots$

An *automaton* is a quadruple $\mathcal{A} = (\Lambda, S, E, I)$ as follows.

- Λ is an alphabet.
- S is a finite set of *states*.
- $I \subset S$ is a set of *initial* states.
- $E \subset S \times \Lambda \times S$ is a set of *transitions*. If $(s, l, s') \in E$, we write $s \xrightarrow{l} s'$.

If for each $(s, l) \in S \times \Lambda$ a transition $s \xrightarrow{l} s'$ exists for at most one $s' \in S$, we will say that the automaton is *weak deterministic*; if such a transition exists for exactly one $s' \in S$, the automaton is *deterministic*. In the other cases, we will call the automaton *non-deterministic*.

A *walk* w in the automaton \mathcal{A} is a finite or infinite sequence of transitions $(s_n, l_n, s'_n)_{n \geq 1}$ such that $s_1 \in I$ and $s'_n = s_{n+1}$. We write

$$w : s_1 \xrightarrow{l_1} s_2 \xrightarrow{l_2} s_3 \xrightarrow{l_3} \dots \quad (3.1)$$

We say that w *starts* from s_1 , and if w is finite of the form $(s_n, l_n, s'_n)_{1 \leq n \leq m}$, we say it *ends* at s'_m . Having two walks w and w' such that w ends where w' starts, we may concatenate them and write $w \& w'$. The associated sequence $l = (l_n)$ of letters of a walk w is the *label* of w . If the automaton is deterministic or weakly deterministic, then the walk w is completely defined by its starting state s_1 and its label l , hence we may simplify the notation and write $w = (s_1; l)$.

As for words, we can define length and prefixes of the walk : the length of w is simply $|w| = |l|$ and a prefix $w|_m$ ($m \leq |w|$) consists of the first m transitions of w :

$$w|_m : s_1 \xrightarrow{l_1} s_2 \xrightarrow{l_2} \dots \xrightarrow{l_m} s_m.$$

Let us recall the construction of the automaton $G(\mathcal{R})$. Let $T = T(\mathbf{M}, \mathcal{D})$ be an integral self-affine \mathbb{Z}^2 -tile. Let e_1, e_2 be the canonical basis of \mathbb{Z}^2 and $R_0 := \{0, \pm e_1, \pm e_2\}$. Define recursively the sets

$$R_n := \{k \in \mathbb{Z}^2; (\mathbf{M}k + \mathcal{D}) \cap (l + \mathcal{D}) \neq \emptyset \text{ for some } l \in R_{n-1}\}$$

and $R := \bigcup_{n \geq 0} R_n \setminus \{0\}$. Then R is a finite set called *contact set* ([8]). It is used to describe the boundary of T . Let $M \subset \mathbb{Z}^2$ and $G(M)$ be the automaton defined as follows. The *states* of $G(M)$ are the elements of M , and for $k, l \in M$, there is a *transition*

$$k \xrightarrow{a|a'} l \quad (a, a' \in \mathcal{D}) \quad \text{iff} \quad \mathbf{M}k + a' = l + a.$$

We may also simply write $k \xrightarrow{a} l$ for such a transition, since a' is then uniquely determined. $G(R)$ is called the *contact automaton* of T . It happens that states of $G(R)$ have no outgoing transitions. Thus we deal with the *reduced* contact automaton. Let $\text{Red}(G(M))$ be the graph emerging from $G(M)$ when all states that are not the starting state of an infinite walk in $G(M)$ are removed. Define \mathcal{R} to be the subset of R such that $\text{Red}(G(R)) = G(\mathcal{R})$. Then, there are non-empty compact sets $(K_s)_{s \in \mathcal{R}}$ such that

$$\partial T = \bigcup_{s \in \mathcal{R}} K_s \quad (3.2)$$

and

$$K_s = \bigcup_{s \xrightarrow{a} s' \in G(\mathcal{R})} \mathbf{M}^{-1}(K_{s'} + a). \quad (3.3)$$

This was proved in [1]. Thus the boundary of T is the attractor of this graph iterated function system (see [7, 18]). $G(\mathcal{R})$ is usually smaller than the boundary GIFS encountered in the literature [11, 13]. Indeed, the set of states of the latter consists of all the *neighbors* of T , that is, the tiles $T + s$ with $T \cap (T + s) \neq \emptyset$. This may be very large if T is not disk-like.

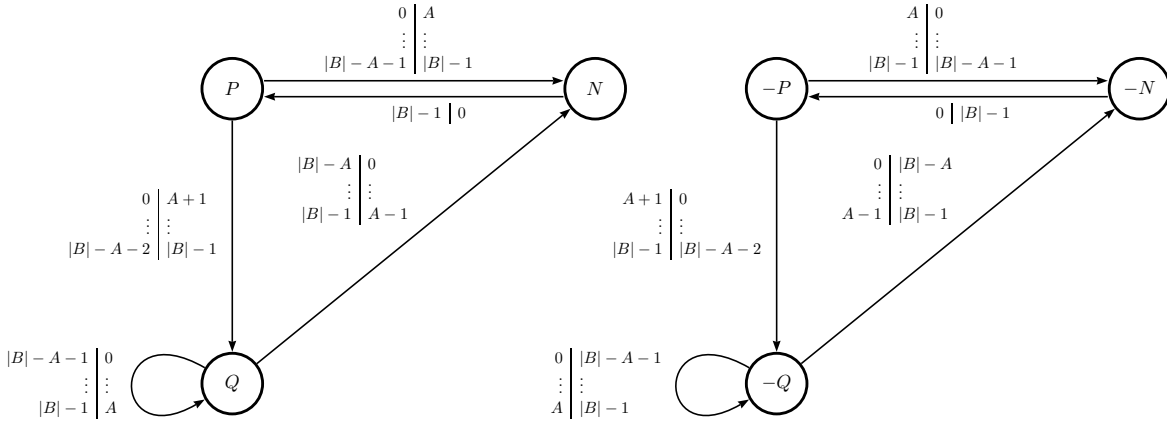
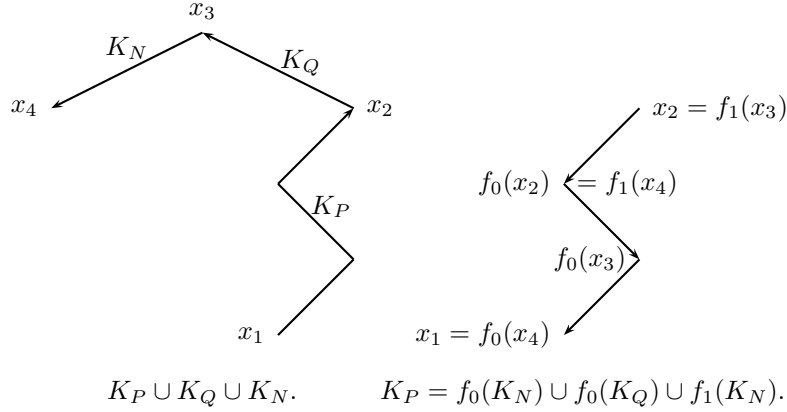
In the remaining part of this section, we suppose that the matrix \mathbf{M} and the digit set \mathcal{D} are as in (2.2), where $A \geq 1$ and $B \leq -3$ (remember that for $A = 0$, T is just a rectangle). In this case,

$$\mathcal{R} = \{\pm P, \pm Q, \pm N\}$$

with

$$P = \begin{pmatrix} 1 \\ 0 \end{pmatrix}, \quad Q = \begin{pmatrix} A+1 \\ 1 \end{pmatrix}, \quad N = \begin{pmatrix} A \\ 1 \end{pmatrix}.$$

The automaton $G(\mathcal{R})$ is depicted on Figure 2. The symmetries in $G(\mathcal{R})$ follow from the fact that $k \xrightarrow{a|a'} l$ if and only if $-k \xrightarrow{a'|a} -l$.

FIGURE 2. Reduced contact automaton $G(\mathcal{R})$ for $A \geq 1, B \leq -3$.FIGURE 3. Flipping for $(A, B) = (2, -4)$.

We now come to the parametrization. We have a surjective mapping

$$\begin{aligned} \psi : G(\mathcal{R}) &\rightarrow \partial T \\ w &\mapsto \sum_{j \geq 1} \mathbf{M}^{-j} a_j, \end{aligned} \quad (3.4)$$

where $w : s_1 \xrightarrow{a_1} s_2 \xrightarrow{a_2} \dots$ is an infinite walk in the automaton $G(\mathcal{R})$. We wish to connect the interval $[0, 1]$ to the boundary ∂T via $G(\mathcal{R})$. This is done by introducing a number system associated to $G(\mathcal{R})$. We proceed in four steps.

Step 1. First note that since $B = \det(\mathbf{M}) < 0$, a flipping occurs. Hence the orientation of the boundary pieces changes at each iteration of (2.4), as explained in Figure 3. The picture shows the flipping for the (roughly represented) boundary part K_P . Since taking \mathbf{M}^2 instead of \mathbf{M} would square the number of digits, we fake the flipping by doubling the number of states.

- For each state $S \in \mathcal{R}$, we create the states S and \bar{S} .
- For each transition $S \xrightarrow{a} T \in G(\mathcal{R})$, we create the transitions $S \xrightarrow{a} \bar{T}$ and $\bar{S} \xrightarrow{a} T$.

The resulting automaton $G'(\mathcal{R})$ is depicted in Figure 4.

Step 2. To define the number system, we need a weak deterministic version of the double sized automaton. This is obtained by ordering its states and transitions. The states are ordered from 1 to 12. The transitions starting from a state i are then ordered from 1 to l_{max} . Note that l_{max} depends on i . We call this ordered extension $G(\mathcal{R})^\circ$. It is depicted in Figure 5. In this figure we kept track of the digits associated to the edges. In this way, the whole set of transitions is an ordered set, from the transition $(1; 1)$ to the transition $(12; l_{max})$. A direct consequence is that for

Step 4. We eventually obtain the number system. The walks $w = (i; o_1, o_2, \dots)$ starting from the state i will be sent to a subinterval of $[0, 1]$ of length u_i . We define the transition function

$$\phi^0(i; o) = \begin{cases} 0, & \text{if } o = 1 \\ \sum_{\substack{1 \leq k < o, \\ i \xrightarrow{k} j}} u_j, & \text{if } o \neq 1. \end{cases}$$

We write $G(\mathcal{R})^{o+}$ when restricting the initial states of $G(\mathcal{R})^o$ to $\{1, \dots, 6\}$. Also, we set $u_0 := 0$.

Proposition 3.1. *Let ϕ be the mapping*

$$\begin{aligned} \phi : G(\mathcal{R})^{o+} &\rightarrow [0, 1] \\ w &\mapsto \lim_{n \rightarrow \infty} (u_0 + u_1 + \dots + u_{i-1} \\ &\quad + \frac{1}{\beta} \phi^0(i; o_1) + \frac{1}{\beta^2} \phi^0(s_1; o_2) + \dots + \frac{1}{\beta^n} \phi^0(s_{n-1}; o_n)) \end{aligned}$$

whenever w is the infinite walk :

$$w : i \xrightarrow{o_1} s_1 \xrightarrow{o_2} \dots \xrightarrow{o_n} s_n \xrightarrow{o_{n+1}} \dots$$

Then ϕ is well-defined, increasing and onto.

The proof of this proposition is straight forward and can be done in the same way as in [1, Proposition 3.2]. The result is also known as Dumont-Thomas number system [6] in the context of substitutive numeration systems. The identifications in this number system play an essential rôle in our construction. Let $w \neq w' \in G(\mathcal{R})^{o+}$, say for example $w >_{lex} w'$. Then $\phi(w) = \phi(w')$ if and only if

$$1. \begin{cases} w = (i + 1; \bar{1}) \\ w' = (i; \bar{l}_{max}) \end{cases} \quad \text{or} \quad 2. \begin{cases} w = (j; o_1, \dots, o_m, o + 1, \bar{1}) \\ w' = (j; o_1, \dots, o_m, o, \bar{l}_{max}) \end{cases} \quad (3.7)$$

holds for some state $i = 1, \dots, 6$ or some prefix $(j; o_1, \dots, o_m)$ and an order o . Thus if $t \in [0, 1]$, $\phi^{-1}(t)$ consists of at most two elements (see also [1, Lemma 3.3]).

We are now ready to connect the interval $[0, 1]$ to ∂T . Let

$$\begin{aligned} \phi^{(1)} : [0, 1] &\rightarrow G(\mathcal{R})^{o+} \\ t &\mapsto \max^{lex} \phi^{-1}(t), \end{aligned} \quad (3.8)$$

where \max^{lex} maps a finite set of walks to its lexicographically maximal walk. Also, we define the natural projection from the ordered extension to the GIFS :

$$\begin{aligned} Pr : G(\mathcal{R})^{o+} &\rightarrow G(\mathcal{R}) \\ (i; o_1, o_2, \dots) &\mapsto I \xrightarrow{a_1} S_1 \xrightarrow{a_2} \dots \end{aligned} \quad (3.9)$$

It can be visualized in Figure 5 via the walk $i \xrightarrow{a_1|o_1} s_1 \xrightarrow{a_2|o_2} \dots$ and the correspondence

$$1, 12 \leftrightarrow P \quad 2, 11 \leftrightarrow Q \quad 3, 10 \leftrightarrow N \quad \dots$$

and so on as in (3.6).

Proposition 3.2. *The mapping $C : [0, 1] \xrightarrow{\phi^{(1)}} G(\mathcal{R})^{o+} \xrightarrow{Pr} G(\mathcal{R}) \xrightarrow{\psi} \partial T$ is onto and Hölder continuous.*

By the correspondence (3.6), the proof will be very similar to the proof given in [1, Propositions 3.4, 3.5]. C is continuous on a dense set, independently of the choice of $G(\mathcal{R})^o$. Our particular choice will give the continuity on the remaining countable part \mathcal{C} of $[0, 1]$. By the GIFS property, it is enough to check the continuity on a finite set of points in \mathcal{C} . This is the purpose of the lemma below. The proof is then inductive.

For the purpose of the proof we extend the definitions of ϕ and Pr to the whole automaton $G(\mathcal{R})^o$.

Lemma 3.3. *The compatibility conditions*

$$\psi(Pr(i; \overline{l_{max}})) = \psi(Pr(i+1; \overline{1})) \quad (1 \leq i \leq 11) \quad (3.10)$$

$$\psi(Pr(12; \overline{l_{max}})) = \psi(Pr(1; \overline{1})) \quad (3.11)$$

$$\psi(Pr(i; \mathbf{o}, \overline{l_{max}})) = \psi(Pr(i; \mathbf{o} + \mathbf{1}, \overline{1})) \quad (1 \leq i \leq 12, 1 \leq o < l_{max}^i) \quad (3.12)$$

$$\psi(Pr(6; \overline{l_{max}})) = \psi(Pr(1; \overline{1})). \quad (3.13)$$

hold.

Proof. Note that the walks in the above equalities end up in cycles in $G(\mathcal{R})^o$. Thus these are finitely many equalities between eventually periodic points. We mentioned in [1] a way to check them by the use of automata. The equalities involve pairs of sequences $(a_n)_{n \geq 1}$ and $(a'_n)_{n \geq 1}$ that lead to the same point :

$$\sum_{n \geq 1} \mathbf{M}^{-n} a_n = \sum_{n \geq 1} \mathbf{M}^{-n} a'_n.$$

The definition of the transitions in $G(\mathcal{R})$ has the following consequence. If the infinite walks

$$\left\{ \begin{array}{l} s \xrightarrow{a_1|a''_1} s_1 \xrightarrow{a_2|a''_2} s_2 \xrightarrow{a_3|a''_3} \dots \\ s \xrightarrow{a'_1|a''_1} s'_1 \xrightarrow{a'_2|a''_2} s'_2 \xrightarrow{a'_3|a''_3} \dots \end{array} \right.$$

exist in $G(\mathcal{R})$, then $\sum_{n \geq 1} \mathbf{M}^{-n} a_n = \sum_{n \geq 1} \mathbf{M}^{-n} a'_n$. In fact, this is an equivalence if one enlarges $G(\mathcal{R})$ to the automaton $G(\mathcal{S})$. Here, $\mathcal{S} \supset \mathcal{R}$ is the set of all neighbors of T (see [1, Section 4]).

Conditions (3.10), (3.11) and (3.13) are easily seen. Indeed, for $i = 1$, we have the equalities :

$$\begin{aligned} Pr(1; \overline{l_{max}}) &= 1 \xrightarrow{|B|-A-1} 10 \xrightarrow{|B|-1} 1 \xrightarrow{|B|-A-1} \dots \\ Pr(2; \overline{1}) &= 2 \xrightarrow{|B|-A-1} 4 \xrightarrow{|B|-1} 6 \xrightarrow{|B|-A-1} \dots \end{aligned}$$

These walks are cycles of length 2 with the same labels. Hence the equality

$$\psi(Pr(1; \overline{l_{max}})) = \psi(Pr(2; \overline{1}))$$

holds trivially. The other cases are treated similarly. Note that (3.13) means $C(0) = C(1)$.

For (3.12), we treat the case $i = 1$. The parity of o ($1 \leq o < l_{max}$) is of importance. If o is odd, then

$$\begin{aligned} Pr(1; o, \overline{l_{max}}) &= 1 \xrightarrow{a} Pr(10; \overline{l_{max}}) \\ Pr(1; o+1, \overline{1}) &= 1 \xrightarrow{a} Pr(11; \overline{1}). \end{aligned}$$

for some digit a . Hence, by (3.10), the equality

$$\psi(Pr(1; o, \overline{l_{max}})) = \psi(Pr(1; o+1, \overline{1}))$$

again holds trivially. If o is even, we have

$$\begin{aligned} Pr(1; o, \overline{l_{max}}) &= 1 \xrightarrow{a} Pr(11; \overline{l_{max}}) \\ Pr(1; o+1, \overline{1}) &= 1 \xrightarrow{a+1} Pr(10; \overline{1}). \end{aligned}$$

for some $a \in \{0, \dots, |B| - A - 2\}$. The label of $Pr(11; \overline{l_{max}})$ is $(a_n)_{n \geq 1} = \overline{(|B| - A - 1)(|B| - 1)}$, and the label of $Pr(10; \overline{1})$ is $(a'_n)_{n \geq 1} = \overline{(|B| - 1)0}$. Hence it remains to check that these digit sequences lead to the same boundary point, that is

$$\sum_{n \geq 1} \mathbf{M}^{-n} a_n = \sum_{n \geq 1} \mathbf{M}^{-n} a'_n.$$

This is because the walks

$$\left\{ \begin{array}{l} P \xrightarrow{a|a''} Q \xrightarrow{|B|-A-1|0} Q \xrightarrow{|B|-1|A} Q \xrightarrow{|B|-A-1|0} \dots \\ P \xrightarrow{a+1|a''} N \xrightarrow{|B|-1|0} P \xrightarrow{0|A} N \xrightarrow{|B|-1|0} \dots \end{array} \right.$$

both exist in $G(\mathcal{R})$ for some digit a'' .

The proof is similar for the other relevant values of i . □

Proof of Proposition 3.2. Let

$$\mathcal{C} := \{t \in [0, 1] ; \quad t = u_0 + u_1 + \dots + u_{i-1} + \frac{1}{\beta} \phi^0(i; o_1) + \frac{1}{\beta^2} \phi^0(s_1; o_2) + \dots + \frac{1}{\beta^m} \phi^0(s_{m-1}; o_m) \\ \text{for some finite walk } i \xrightarrow{a_1|o_1} s_1 \xrightarrow{a_2|o_2} \dots \xrightarrow{a_m|o_m} s_m \in G(\mathcal{R})^o\}.$$

Then it can be shown that C is continuous on \mathcal{C} , right continuous on $[0, 1] \setminus \mathcal{C}$ and that $\lim_{t^-} C$ exists also for all $t \in [0, 1] \setminus \mathcal{C}$. These properties would be valid for any ordering of the automaton. But our special choice of $G(\mathcal{R})^o$ has also left continuity properties. Lemma 3.3 implies the left continuity of C at the points associated to walks of length $m = 0$ and $m = 1$ in the definition of \mathcal{C} . Let now $t \in \mathcal{C}$ associated to a walk of length $m \geq 2$ but not to a walk of smaller length. Thus

$$t = \phi(\underbrace{i; o_1, \dots, o_m, \bar{1}}_w)$$

with $o_m \neq 1$. We write (a_1, a_2, \dots) for the labeling sequence of $Pr(w)$. Also, we write $f_a(x) := \mathbf{M}^{-1}(x + a)$. Then,

$$\begin{aligned} C(t) &= \psi(Pr(w)) = f_{a_1} \circ \dots \circ f_{a_m} \circ \psi(Pr(j; o_m, \bar{1})) \\ &= f_{a_1} \circ \dots \circ f_{a_m} \circ \psi(Pr(j; o_m - 1, \overline{l_{max}})) \quad (\text{by Condition (3.12)}) \\ &= C(t^-) \end{aligned}$$

(here j is the ending state of the walk $w|_{m-1}$ in the automaton $G(\mathcal{R})^o$). Thus C is left continuous in t .

The Hölder continuity is then a consequence of the left continuity. It can be proved as in [1]. \square

We finally give the sequence of polygonal approximations associated to the above parametrization and prove that they are simple closed curves.

Let $C : [0, 1] \rightarrow \partial T$ be the parametrization of Proposition 3.2. For N points M_1, \dots, M_N of \mathbb{R}^d , we denote by $[M_1, \dots, M_N]$ the curve joining M_1, \dots, M_N in this order by straight lines.

Let $w_1^{(n)}, \dots, w_{N_n}^{(n)}$ be the finite walks of length n of the automaton $G(\mathcal{R})^{o+}$ in the lexicographical order :

$$(1; 1, \dots, 1) = w_1^{(n)} \leq_{lex} w_2^{(n)} \leq_{lex} \dots \leq_{lex} w_{N_n}^{(n)} = (6; l_{max}, \dots, l_{max}),$$

where N_n is the number of these walks. For $n = 0$, these are just the states $1, \dots, 6$. Let

$$C_j^{(n)} := C(\phi(w_j^{(n)} \& \bar{1})) \in \partial T \quad (1 \leq j \leq N_n).$$

Then we call

$$\Delta_n := [C_1^{(n)}, C_2^{(n)}, \dots, C_{N_n}^{(n)}, C_1^{(n)}],$$

the n -th approximation of ∂T .

We will need the following lemmas. The first one interprets these approximations as the iterated sequence of the GIFS $G(\mathcal{R})$. We write $G(\mathcal{R})_n^{o+}(i)$ for the walks of length n starting from the state i . Also, for w of length n , we write w^{+1} the next walk in the lexicographical order. We make the convention that the maximal walk has the minimal one as follower. For $i = 1 \dots 6$, let

$$\Delta_i^{(n)} := \bigcup_{w \in G(\mathcal{R})_n^{o+}(i)} [C(\phi(w \& \bar{1})), C(\phi(w^{+1} \& \bar{1}))].$$

Lemma 3.4. For all $n \in \mathbb{N}$,

$$\begin{cases} \Delta_n &= \bigcup_{i=1}^6 \Delta_i^{(n)} \\ \Delta_i^{(n+1)} &= \bigcup_{i \xrightarrow{a} j \in G(\mathcal{R})} \mathbf{M}^{-1}(\Delta_j^{(n)} + a). \end{cases} \quad (3.14)$$

Proof. This is a consequence of the left continuity of the parametrization. The proof is inductive. Note that

$$Pr(j; \bar{1}) = Pr(13 - j; \overline{l_{max}})$$

for all $j = 1, \dots, 6$ by construction of $G(\mathcal{R})^\circ$. Therefore,

$$\begin{aligned}
\bigcup_{i \xrightarrow{a} j \in G(\mathcal{R})} f_a(\Delta_j^{(0)}) &= \bigcup_{i \xrightarrow{a|o} 13-j \in G(\mathcal{R})^{\circ+(i)}} f_a([\psi(\text{Pr}(13-j; \overline{l_{max}})), \psi(\text{Pr}(12-j; \overline{l_{max}}))]) \\
&= \bigcup_{i \xrightarrow{a|o} 13-j} f_a([\psi(\text{Pr}(13-j; \overline{l_{max}})), \psi(\text{Pr}(13-j; \overline{1}))]) \text{ by (3.10)} \\
&= \bigcup_{i \xrightarrow{a|o} 13-j} [\psi(\text{Pr}(i; o, \overline{l_{max}})), \psi(\text{Pr}(i; o, \overline{1}))] \\
&= \bigcup_{i \xrightarrow{a|o} j \in \left[\begin{array}{l} \psi(\text{Pr}(w^{+1} \& \overline{1})), \psi(\text{Pr}(i; o, \overline{1})) \\ \underbrace{\hspace{1.5cm}}_w \end{array} \right]} \text{ by (3.12)} \\
&= \Delta_i^{(1)}.
\end{aligned}$$

The induction step goes similarly. \square

The second lemma exhibits a tiling of the plane by hexagons naturally associated to the parametrization. will simply write C_1, \dots, C_6 instead of $C_1^{(0)}, \dots, C_6^{(0)}$. Hence we have:

$$\begin{aligned}
C_1 &= \psi(\overline{0(|B|-1)}), & C_2 &= \psi(\overline{(|B|-A-1)(|B|-1)}), & C_3 &= \psi(\overline{(|B|-1)(|B|-A-1)}), \\
C_4 &= \psi(\overline{(|B|-1)0}), & C_5 &= \psi(\overline{A0}), & C_6 &= \psi(\overline{0A}).
\end{aligned} \tag{3.15}$$

Lemma 3.5. $[C_1, \dots, C_6, C_1]$ is a simple closed curve. Let Q be the closure of its bounded complementary component. Then $Q + \mathbb{Z}^2$ is a tiling of the plane. Two neighboring tiles have 1-dimensional intersection. Moreover, the neighbors of Q are the tiles $Q + s$ with $s \in \mathcal{R}$, that is,

$$\partial Q = \bigcup_{s \in \mathcal{R}} Q \cap (Q + s).$$

Proof. The proof is similar as in [1, Proposition 5.5]. The coordinates of the vertices of Q can be computed as rational expressions in A, B . The following relations hold.

$$C_3 = C_1 + (A, 0), \quad C_4 = C_6 + (A, 1), \quad C_2 = C_4 + (1, 0), \quad C_1 = C_5 + (1, 0). \tag{3.16}$$

Moreover, $C_6 - C_5 = (\frac{(A-1)A}{|B|+1-A}, \frac{A}{|B|+1-A})$. This gives the relative position of the vertices and the lemma then follows from geometrical considerations. \square

We define the natural approximations of T , when starting with the polygon Q . Let $T_0 := Q$, the hexagon of the above proposition and for all $n \geq 0$,

$$\mathbf{M}T_{n+1} = \bigcup_{a \in \mathcal{D}} (T_n + a).$$

By the preceding lemma, $\mathbf{M}^n T_n$ is a union of $|\mathcal{D}|^n$ hexagons congruent to Q . Since two neighboring hexagons have a one dimensional intersection, this union is disk-like (see [1, Proposition 5.6]). Moreover, the equality

$$\Delta_n = \partial T_n \tag{3.17}$$

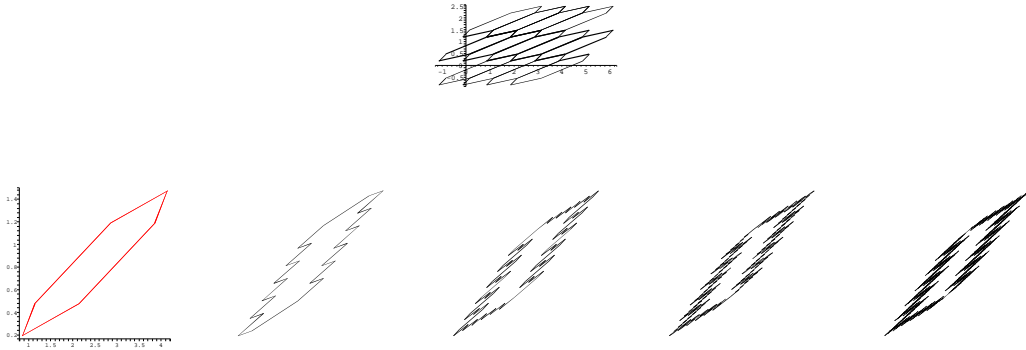
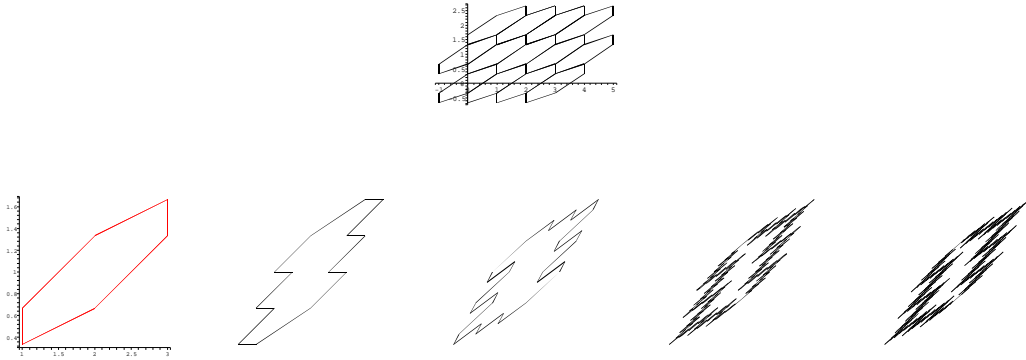
holds for all n . It was proved in [1] by showing that ∂T_n fulfills the same recurrence relation as Δ_n , given here in Lemma 3.4. Thus Δ_n is a simple closed curve.

This leads to the following proposition.

Proposition 3.6. Δ_n is a simple closed polygonal curve and its vertices have $\mathbb{Q}(\beta)$ -addresses. Moreover, (Δ_n) converges to ∂T in Hausdorff metric.

Proof. By definition, Δ_n is a closed polygonal curve. The vertices have $\mathbb{Q}(\beta)$ -addresses, since they correspond to the finite sums in Proposition 3.1. The convergence in Hausdorff metric follows from Lemma 3.4, since ∂T is the attractor of the GIFS $G(\mathcal{R})$. The fact that Δ_n is a simple curve follows from its equality to ∂T_n . \square

Examples of the polygonal tiling and the approximation sequences are given in Figure 6 (disk-like tile) and Figure 7 (non disk-like tile).

FIGURE 6. $A = 2, B = -6$: polygonal tiling, $\Delta_0, \dots, \Delta_4$ FIGURE 7. $A = 1, B = -3$: polygonal tiling, Δ_i ($i = 0, 1, 2, 5, 6$).

4. THE RELATION TO THE RECURRENT SET METHOD

The recurrent set method was introduced in [4, 5]. It produces fractal curves from a given substitution and an embedding into the plane. An assumption called short range cancellation is required for the substitution. A fractal curve obtained in this way is the boundary of a self-similar tile. Conversely, given a self-similar tile, it may not be easy to find an associated boundary substitution satisfying short range cancellation and the appropriate embedding. For example, the class of self-similar tiles produced by substitutions on two letters was characterized in [22]. We will show that our class can entirely be described via the recurrent set method by substitutions on three letters.

Let $T = T(\mathbf{M}, \mathcal{D})$ be defined by the matrix \mathbf{M} and the digit set \mathcal{D} as in (2.2). We treat the case $A > 0, B < 0$. A substitution is read off from the ordered contact automaton. It is the endomorphism of the free group over three letters $\langle a, b, c \rangle$, first defined for a, b, c according to Figure 5:

$$\begin{aligned} a &\rightarrow (\dot{c}\dot{b})^{|B|-A-1}\dot{c} \\ b &\rightarrow (\dot{b}\dot{c})^A\dot{b} \\ c &\rightarrow \dot{a} \end{aligned}$$

where $\dot{a}, \dot{b}, \dot{c}$ stand for the inverses of the letters a, b, c . This definition is then extended to $\langle a, b, c \rangle$ by concatenation. We call this substitution σ .

Remark 4.1. The original twelve letters are reduced to six (a, b, c and their inverses). This is because there will be three directions, along which we will draw the curves in the plane. Firstly, a, b, c are associated to 1, 2, 3, and $\dot{a}, \dot{b}, \dot{c}$ to 4, 5, 6, since the underlying elements of \mathcal{R} are exactly $P, Q, N, -P, -Q, -N$. Secondly, 7, 8, 9, 10, 11, 12 are associated to $c, b, a, \dot{c}, \dot{b}, \dot{a}$ respectively, as the states 7, \dots , 12 are redundancies to fake the flipping (i and $13 - i$ give the same direction but reverse orientation).

Let Q be the hexagon whose vertices C_1, \dots, C_6 were defined in (3.15). We proved in Lemma 3.5 that $Q + \mathbb{Z}^2$ is a tiling of the plane. This allows us to construct directed curves in the plane as follows. Let

$$\begin{aligned} \mathbf{v}_a &:= C_2 - C_1, & \mathbf{v}_b &:= C_3 - C_2, & \mathbf{v}_c &:= C_4 - C_3, \\ \mathbf{v}_{\dot{a}} &:= C_5 - C_4 = -\mathbf{v}_a, & \mathbf{v}_{\dot{b}} &:= C_6 - C_1 = -\mathbf{v}_b, & \mathbf{v}_{\dot{c}} &:= C_1 - C_6 = -\mathbf{v}_c, \end{aligned}$$

and g the homomorphism

$$\begin{aligned} g : \langle a, b, c \rangle &\rightarrow \mathbb{R}^2 \\ o_1 o_2 \dots o_n &\rightarrow \mathbf{v}_{o_1} + \dots + \mathbf{v}_{o_n}. \end{aligned}$$

The important property of g is that it connects the action of σ on the words and the action of \mathbf{M} on the plane. More precisely, for all words $w \in \langle a, b, c \rangle$,

$$g(\sigma(w)) = \mathbf{M}g(w). \quad (4.1)$$

Given a reduced word $a_1 \dots a_m$, let $p(a_1 \dots a_m)$ stand for the polygonal path joining

$$0, g(a_1), g(a_1 a_2), \dots, g(a_1 \dots a_m)$$

in this order by straight lines. So if $W_0 := abc\dot{a}\dot{b}\dot{c}$, then the curve $p(W_0)$ is the boundary of the hexagon Q up to a translation by $-C_1$. We say that a directed curve *encloses clockwise* (resp. *counterclockwise*) a bounded set Q_0 if it is a simple closed curve oriented clockwise (resp. counterclockwise) and equal to the boundary of Q_0 .

Proposition 4.2. *For all $n \geq 1$, $p(\sigma^n(W_0))$ encloses*

$$Q - C_1 + \sum_{k=0}^{n-1} g(\sigma^k(\dot{a}bc)) + \mathcal{D} + \dots + \mathbf{M}^{n-1}\mathcal{D},$$

clockwise if n is odd and counterclockwise if n is even.

Proof. The inductive proof runs as [1, Proposition 6.2].

First note that $p(W_0) = p(abc\dot{a}\dot{b}\dot{c})$ encloses $Q - C_1$ counter-clockwise. For $n = 1$,

$$\begin{aligned} p(\sigma(abc\dot{a}\dot{b}\dot{c})) &= p((\dot{c}\dot{b})^{|\mathcal{B}|} \dot{a}(cb)^{|\mathcal{B}|} a) \\ &= p(\dot{a}a(\dot{c}\dot{b}aa)^{|\mathcal{B}|-1} \dot{c}\dot{b}\dot{a}(cb)^{|\mathcal{B}|} a) \\ &= p(\dot{a}(a\dot{c}\dot{b}\dot{a})^{|\mathcal{B}|} (cb)^{|\mathcal{B}|} a) \\ &= g(\dot{a}) + \bigcup_{x=0}^{|\mathcal{B}|-1} \left[p(a\dot{c}\dot{b}\dot{a}cb) + xg(a\dot{c}\dot{b}\dot{a}) \right] \setminus \bigcup_{x=1}^{|\mathcal{B}|-1} \left[p(\dot{a}) + xg(a\dot{c}\dot{b}\dot{a}) \right] \\ &= g(\dot{a}) + \bigcup_{x=0}^{|\mathcal{B}|-1} \left[p(a\dot{c}\dot{b}\dot{a}cb) + \begin{pmatrix} x \\ 0 \end{pmatrix} \right] \setminus \bigcup_{x=1}^{|\mathcal{B}|-1} \left[p(\dot{a}) + \begin{pmatrix} x \\ 0 \end{pmatrix} \right]. \end{aligned}$$

We made a slight abuse of notation : the endpoints of the translates of $p(\dot{a})$ are in fact included in the curve $p(\sigma(abc\dot{a}\dot{b}\dot{c}))$. Each $p(a\dot{c}\dot{b}\dot{a}cb) + \begin{pmatrix} x \\ 0 \end{pmatrix}$ encloses clockwise the boundary of the hexagon

$$Q - C_1 + g(cb) + \begin{pmatrix} x \\ 0 \end{pmatrix},$$

and these hexagons are essentially disjoint by the tiling property of Q . Thus $p(\sigma(abc\dot{a}\dot{b}\dot{c}))$ is the boundary of the union $Q - C_1 + g(\dot{a}cb) + \mathcal{D}$ of hexagons glued together through the edges $p(\dot{a}) + \begin{pmatrix} x \\ 0 \end{pmatrix}$. The intersections are one-dimensional. In other words, $p(\sigma(abc\dot{a}\dot{b}\dot{c}))$ encloses $Q - C_1 + g(\dot{a}bc) + \mathcal{D}$.

Suppose now the statement true for some $n \geq 1$. Then

$$\begin{aligned} p(\sigma^{n+1}(abc\dot{a}\dot{b}\dot{c})) &= p(\sigma^n(\dot{a}a(\dot{c}\dot{b}\dot{a}a)^{|B|}\dot{a}(cb)^{|B|}a)) \\ &= p((\sigma^n(\dot{a}(a\dot{c}\dot{b}\dot{a}))^{|B|}(cb)^{|B|}a)) \\ &= g(\sigma^n(\dot{a})) + \bigcup_{x=0}^{|B|-1} \left[p(\sigma^n(ac\dot{b}\dot{a}cb)) + xg(\sigma^n(ac\dot{b}\dot{a})) \right] \\ &\quad \setminus \bigcup_{x=1}^{|B|-1} \left[p(\sigma^n(\dot{a})) + xg(\sigma^n(ac\dot{b}\dot{a})) \right] \end{aligned}$$

Using the induction hypothesis and the equality (4.1), it follows that $p(\sigma^{n+1}(abc\dot{a}\dot{b}\dot{c}))$ encloses the union of tiles

$$Q - C_1 + \mathcal{D} + \dots + \mathbf{M}^n \mathcal{D} + g(\dot{a}bc) + \dots + g(\sigma^{n-1}(\dot{a}bc)) + g(\sigma^n(\dot{a}bc))$$

(clockwise or counter-clockwise, depending on the parity of n), and we are done. \square

5. THE OTHER CASES

In this section, we show that the previous construction of parametrization holds for the whole class and we characterize the disk-like cases. Theorems 1, 2 and 3 were proved for $B > 0, A > 0$ in [1] and will follow from the results of Sections 3 and 4 for $B < 0, A > 0$. The remaining cases are easily seen as a consequence of (2.11). However, it just gives the existence of the corresponding parametrization for the latter two cases. By proving Proposition 2.1, we want to make sure that our method is efficient to produce directly these parametrizations.

We give the meaning of symmetric ordered extension G^O . Every state of an ordered extension G^O of $G(\mathcal{R})$ is associated to a state $s \in \mathcal{R}$ (sometime via \bar{s} in the case $B < 0$). We call G^O *symmetric* if the transitions

$$\begin{aligned} (B > 0) \quad & s \xrightarrow{a} s' \text{ and } -s \xrightarrow{|B|-1-a} -s' \text{ are given the same order } \mathbf{o}. \\ (B < 0) \quad & s \xrightarrow{a} \bar{s}' \text{ and } -s \xrightarrow{|B|-1-a} \overline{-s'} \text{ (as well as } \bar{s} \xrightarrow{a} s' \text{ and } \overline{-s} \xrightarrow{|B|-1-a} -s' \text{)} \\ & \text{are given the same order } \mathbf{o}. \end{aligned} \quad (5.1)$$

Proof of Proposition 2.1. We construct the extension G_2^O . The main property we use is the following. Remember that $s \xrightarrow{a|a'} s'$ ($s, s' \in \mathcal{R}$) is a transition in the reduced automaton $G(\mathcal{R})$ if and only if $\mathbf{M}s + a' = s' + a$. \mathcal{R} is symmetric, that is, $\mathcal{R} = -\mathcal{R}$. Moreover,

$$\begin{aligned} s \xrightarrow{a} s' \in G_1(\mathcal{R}_1) &\iff -s \xrightarrow{|B|-1-a} -s' \in G_1(\mathcal{R}_1) \\ \iff -\mathbf{P}s \xrightarrow{a} \mathbf{P}s' \in G_2(\mathcal{R}_2) &\iff \mathbf{P}s \xrightarrow{|B|-1-a} -\mathbf{P}s' \in G_2(\mathcal{R}_2) \end{aligned} \quad (5.2)$$

This can be seen from the construction of $G(\mathcal{R})$ (Section 3).

We now build up G_2^O by introducing an order on G_2 as follows. Suppose first that $B > 0$, that is, $G_1 = G_1(\mathcal{R}_1)$ and $G_2 = G_2(\mathcal{R}_2)$. Since $\mathcal{R}_2 = \mathbf{P}\mathcal{R}_1$, we naturally transfer the order chosen for \mathcal{R}_1 to \mathcal{R}_2 :

$$s \leftrightarrow i \quad \longmapsto \quad \mathbf{P}s \leftrightarrow i \quad (5.3)$$

However, we transfer the transitions $(i; \mathbf{o})$ of G_1^O to transitions of G_2^O in a different manner:

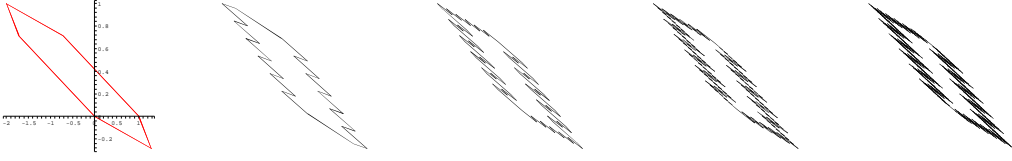
$$s \xrightarrow{a} t \leftrightarrow i \xrightarrow{a|\mathbf{o}} j \quad \longmapsto \quad \mathbf{P}s \xrightarrow{|B|-1-a} -\mathbf{P}t \leftrightarrow i \xrightarrow{|B|-1-a|\mathbf{o}} j' \in G_2^O \quad (5.4)$$

(thus j' is defined via $\mathbf{P}(-t) \leftrightarrow j'$). We prove that if $w = (i; \mathbf{o}_1, \mathbf{o}_2, \dots)$ is a walk in G_1^O , then it is also a walk in G_2^O . Let us write

$$Pr_1(w) = s \xrightarrow{a_1} s_1 \xrightarrow{a_2} s_2 \xrightarrow{a_3} \dots \in G_1.$$

Then the walk

$$w' := \mathbf{P}s^i \xrightarrow{|B|-1-a_1} -\mathbf{P}s_1 \xrightarrow{a_2} \mathbf{P}s_2 \xrightarrow{|B|-1-a_3} \dots \in G_2.$$

FIGURE 8. $A = -2, B = -6$: polygonal tiling, $\Delta_0, \dots, \Delta_4$

This is a consequence of (5.2). It now follows from (5.4) and the assumption of symmetry of the ordered extension G_1^O that

$$i \xrightarrow{|B|-1-a_1|\mathbf{o}_1} j'_1 \xrightarrow{a_2|\mathbf{o}_2} j_2 \xrightarrow{|B|-1-a_3|\mathbf{o}_3} \dots \in G_2^O.$$

This argument even shows a one to one correspondence between G_1^O and G_2^O . Moreover, let Pr_2 the natural projection from G_2^O to G_2 and ψ_2 the boundary mapping. Then

$$\begin{array}{ccccccc} G_1^O & \xrightarrow{id} & G_2^O & \xrightarrow{Pr_2} & G_2 & \xrightarrow{\psi_2} & \partial T_2 \\ w & \mapsto & w & \mapsto & w' & \mapsto & \psi_2(w'), \end{array}$$

where

$$\begin{aligned} \psi_2(w') &= \mathbf{M}^{-1} \begin{pmatrix} |B| - 1 - a_1 \\ 0 \end{pmatrix} + \mathbf{M}^{-2} \begin{pmatrix} a_2 \\ 0 \end{pmatrix} + \mathbf{M}^{-3} \begin{pmatrix} |B| - 1 - a_3 \\ 0 \end{pmatrix} + \dots \\ &= \mathbf{P}\psi_1((Pr_1(w)) + \mathbf{v}). \end{aligned}$$

The case of $B < 0$ is treated similarly. □

Remark 5.1. The consequences of this proposition are that :

- (1) the compatibility conditions (2.7) to (2.9) are equivalently fulfilled by G_1^O and G_2^O ;
- (2) the same (Dumont Thomas-like) number system is associated to G_1^O and G_2^O .

We are now able to prove all our theorems.

Proof of Theorem 1. The theorem is a direct consequence of the previous sections for the case ($A \geq 1, B \leq -3$). Indeed, by Proposition 3.2, we obtain a Hölder continuous parametrization $C : [0, 1] \rightarrow \partial T$, and Lemma 3.5 gives the corresponding hexagon Q . Equality (3.17) together with Proposition 3.6 insure that the parametrization and the associated sequence of approximations have the required properties (1),(2),(3) of the theorem.

The symmetric case ($A \leq -1, B \leq -3$) follows from Proposition 2.1, with the simple relation $C(t) = f(C'(t))$ between two parametrizations C for (A, B) and C' for $(-A, B)$ ($A \leq -1$). The proof for ($A \geq 1, B \geq 2$) was given in [1, Theorem 4] and again the symmetric case ($A \leq -1, B \geq 2$) follows from Proposition 2.1. □

Figure 8 represents the case $A = -2, B = -6$. It can be also obtained from Figure 6 after reflection by x -axis and translation.

Proof of Theorem 2. The theorem was proved in [1, Theorem 2] in the case that the contact automaton $G(\mathcal{R})$ is strongly connected. It is an application of [9, 17] that mainly relies on an open set condition for the GIFS (see also [1, Proposition 3.13]).

Note that for ($A \geq 1, B \leq -3$) the automaton $G(\mathcal{R})$ is disconnected and consists of two strongly connected components (see Figure 2). These two components have the same incidence matrix. Thus the results apply separately on each component for a common generalized Hausdorff

measure. Let β the Perron Frobenius eigenvalue associated to the components of $G(\mathcal{R})$, as in *Step 3* of Section 3. Let \mathcal{H}_w^α , where

$$\alpha := 2 \frac{\log(\beta)}{\log(|\det(\mathbf{M})|)}.$$

Then we have $\infty > \mathcal{H}_w^\alpha(K_s) > 0$ for each boundary part K_s ($s \in \mathcal{R}$). Moreover, there is a separation property :

$$\mathcal{H}_w^\alpha(K_s) = \frac{1}{\beta} \sum_{s \xrightarrow{\alpha} s' \in G(\mathcal{R})} \mathcal{H}_w^\alpha(K_{s'}).$$

This remains true for the attractor $(K_i)_{1 \leq i \leq 12}$ of the duplicated automaton of Figures 5, because of the correspondence (3.6). The proof then runs as in [1].

The case $(A \geq 1, B \geq 2)$ is part of [1, Theorem 4]. The remaining symmetric cases (for $A \leq -1$) are a consequence of Proposition 2.1. \square

We mention that, for $(A \geq 1, B \geq 2)$, we even proved in [1] the measure disjointness of the boundary parts K_s ($s \in \mathcal{R}$). In this case, the description reads as follows :

$$\frac{1}{c} \mathcal{H}_w^\alpha (C([0, t])) = t \quad (t \in [0, 1])$$

with $c = \mathcal{H}_w^\alpha(\partial T)$. The reason is that each intersection $K_s \cap K_{s'}$ appeared in a smaller scale inside some other boundary part $K_{s''}$. By symmetry, this description holds also for $(A \leq -1, B \geq 2)$. For the other cases, a more detailed study of the triple intersections would be necessary.

Proof of Theorem 3. The case $(A \geq 1, B \leq -3)$ is a consequence of Proposition 4.2. Indeed, $\mathbf{M}^{-n}p(\sigma^n(W_0))$ encloses

$$\mathbf{M}^{-n}Q - \mathbf{M}^{-n}C_1 + \mathbf{M}^{-n} \sum_{k=0}^{n-1} g(\sigma^k(\dot{abc})) + \mathbf{M}^{-n}\mathcal{D} + \dots + \mathbf{M}^{-1}\mathcal{D},$$

that is,

$$\mathbf{M}^{-n}p(\sigma^n(W_0)) = \partial T_n + \mathbf{k}_n,$$

where $\mathbf{k}_n = -\mathbf{M}^{-n}C_1 + \sum_{k=1}^n \mathbf{M}^{-k}g(\dot{abc})$. This gives the first equality of the theorem. Therefore, the second equality holds, since $(\partial T_n)_{n \geq 0}$ converges to ∂T and $(\mathbf{k}_n)_{n \geq 0}$ converges to

$$\mathbf{k} = \sum_{k=1}^{\infty} \mathbf{M}^{-k}g(\dot{abc}).$$

Let now (A, B) satisfy $A \leq -1$ and $B \leq -3$. Let C be the boundary parametrization of the corresponding tile, and C' of the tile associated to the symmetric case $(-A, B)$. Then, by Proposition 2.1, $C(t) = f(C'(t))$. Note that f contains a reflection with respect to the x -axis. Thus a statement similar to Proposition 4.2 holds, after exchanging clockwise and counterclockwise. It follows that Theorem 3 holds in the same manner as above.

The case $(A \geq 1, B \geq 3)$ was treated in [1, Section 6] and the symmetric case $(A \leq -1, B \geq 3)$ follows again from Proposition 2.1. \square

In [16], the disk-like tiles $T(\mathbf{M}, \mathcal{D})$ among our class were completely characterized. We are able to give a new proof of this statement, by showing that the corresponding boundary parametrization $C : [0, 1] \rightarrow \partial T$ is injective (up to $C(0) = C(1)$).

Proposition 5.2 (see [16]). *Let \mathbf{M}_0 have characteristic polynomial $x^2 + Ax + B$ and*

$$\mathcal{D}_0 = \{0, v, 2v, \dots, (|B| - 1)v\}$$

for some $v \in \mathbb{Z}^2$ such that $v, \mathbf{M}_0 v$ are linearly independent. Let $T = T(\mathbf{M}_0, \mathcal{D}_0)$ be the tile defined by $\mathbf{M}_0 T = T + \mathcal{D}_0$. Then T is homeomorphic to a disk if and only if $2|A| \leq |B + 2|$.

Proof. As noticed in Section 2, $T(\mathbf{M}_0, \mathcal{D}_0) = \mathbf{C}T(\mathbf{M}, \mathcal{D})$, where \mathbf{C} is an invertible matrix and $(\mathbf{M}, \mathcal{D})$ is as in (2.2). Thus we just prove the statement for the latter subclass. Suppose that $A \geq 1$ and $B \leq -3$. Let C be the parametrization of ∂T constructed in Section 3, in particular Proposition 3.2 :

$$C : [0, 1] \xrightarrow{\phi^{(1)}} G(\mathcal{R})^{o+} \xrightarrow{Pr} G(\mathcal{R}) \xrightarrow{\psi} \partial T.$$

Remember that $\phi^{(1)}$ is a reciprocal of $\phi : G(\mathcal{R})^{o+} \rightarrow [0, 1]$ (Proposition 3.1).

We wonder for which choice of (A, B) the curve ∂T is a simple closed curve, that is, the parametrization C is injective. The pairs of identified walks

$$\{(w, w') \in G(\mathcal{R})^o \times G(\mathcal{R})^o ; w \neq w', \phi(w) = \phi(w')\}$$

are given by Equation (3.7). They give rise to an automaton \mathcal{A}^ϕ (see [1, Proposition 4.1]), depicted on Figure 9. In this figure, a walk is admissible if it starts from a colored state (*initial state*) and passes through a double circled state (*final state*) infinitely many times. The admissible walks W in Figure 9

$$W : s|s' \xrightarrow{a_1|o_1 \parallel a'_1|o'_1} s_1|s'_1 \xrightarrow{a_2|o_2 \parallel a'_2|o'_2} \dots$$

consist exactly in the pairs $w|w'$ of walks in $G(\mathcal{R})^{o+}$:

$$w : s \xrightarrow{a_1|o_1} s_1 \xrightarrow{a_2|o_2} \dots$$

and

$$w' : s' \xrightarrow{a'_1|o'_1} s'_1 \xrightarrow{a'_2|o'_2} \dots$$

for which $\phi(w) = \phi(w')$ (and $w \geq_{lex} w'$, for simplicity). Since the core of the automaton is $G(\mathcal{R})^{o+}$, we did not represent the transitions. In this part, the two walks w, w' do not yet distinguish.

We proved that such pairs lead to the same boundary point :

$$\phi(w) = \phi(w') \Rightarrow \psi(Pr(w)) = \psi(Pr(w')).$$

This insured the continuity of C . Thus they are included in the set of pairs

$$\{(w, w') \in G(\mathcal{R})^o \times G(\mathcal{R})^o ; w \neq w', \psi(Pr(w)) = \psi(Pr(w'))\}.$$

Note that C is injective if and only if both set of pairs are equal, that is if and only if

$$\phi(w) = \phi(w') \Leftrightarrow \psi(Pr(w)) = \psi(Pr(w')).$$

The latter pairs can also be read off from an automaton. This property was shown in [1, Propositions 4.2, 4.5] and follows from the following fact. Let $\mathcal{S} := \{s \in \mathbb{Z}^2 ; s \neq 0, T \cap (T+s) \neq \emptyset\}$ be the set of neighbors of T . As mentioned in the proof of Lemma 3.3,

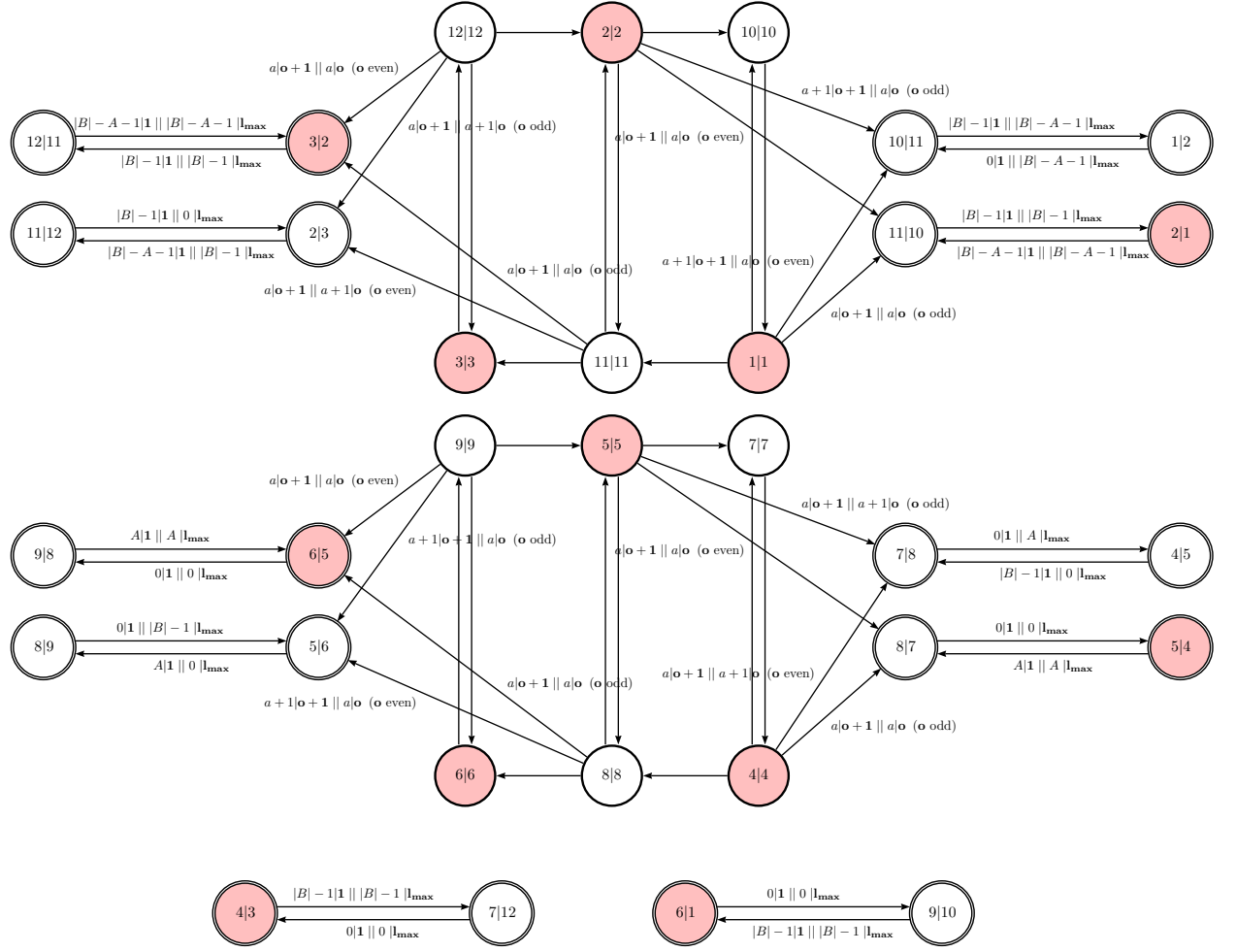
$$\sum_{n \geq 1} \mathbf{M}^{-n} a_n = \sum_{n \geq 1} \mathbf{M}^{-n} a'_n \in \partial T$$

if and only if two infinite walks

$$\left\{ \begin{array}{l} s \xrightarrow{a_1|a'_1} s_1 \xrightarrow{a_2|a'_2} s_2 \xrightarrow{a_3|a'_3} \dots \\ s \xrightarrow{a'_1|a''_1} s'_1 \xrightarrow{a'_2|a''_2} s'_2 \xrightarrow{a'_3|a''_3} \dots \end{array} \right.$$

exist in $G(\mathcal{S})$. Pulling back these walks to the ordered automaton, one obtains all the pairs (w, w') of walks of $G(\mathcal{R})^{o+}$ representing the same boundary point. This splits into two automata : \mathcal{A}^ψ , for which $(a_n)_{n \geq 1} \neq (a'_n)_{n \geq 1}$, and \mathcal{A}^{sl} , for which the walks w, w' in $G(\mathcal{R})^{o+}$ carry the same digit labels $(a_n)_{n \geq 1}$.

Suppose that $2A \leq -B - 2$. Using techniques of [19], one can compute that $\mathcal{R} = \mathcal{S}$. Thus in this case $G(\mathcal{R}) = G(\mathcal{S})$ is the automaton depicted in Figure 2. The automata \mathcal{A}^ψ and \mathcal{A}^{sl} are then easily computed and depicted in Figures 10 and 11. Since their union produces the same sets of pairs as \mathcal{A}^ϕ , it follows that the corresponding boundary parametrization C is injective, thus T is disk-like.

FIGURE 9. \mathcal{A}^ϕ for $A \geq 1, B \leq -3$.

On the contrary, if $2A > -B - 2$, then one can find $t \neq t' \in (0, 1)$ such that $C(t) = C(t')$. Indeed, in this case, $|B| - A - 1 \leq A$. Thus the following walks in $G(\mathcal{R})^{\circ+}$ (Figure 5) exist :

$$w : 2 \xrightarrow{|B|-A-1|\mathbf{1}} 11 \xrightarrow{|B|-A-1|\mathbf{l}_{\max}} |B|-A-1|\mathbf{1} \xrightarrow{\dots},$$

$$w' : 5 \xrightarrow{|B|-A-1|\mathbf{o}} 8 \xrightarrow{|B|-A-1|\mathbf{o}'} 5 \xrightarrow{|B|-A-1|\mathbf{o}} \dots$$

for some orders \mathbf{o}, \mathbf{o}' . Then $\psi(\text{Pr}(w)) = \psi(\text{Pr}(w'))$ holds trivially, whereas obviously

$$t := \phi(w) < \phi(w') =: t'.$$

It follows that C has a double point, thus ∂T can not be a simple closed curve and T is not disk-like.

Since changing A to $-A$ does not change the topology of the corresponding tile (Equality (2.11)), we have for $A \leq -1, B \leq -3$ that T is disk-like if and only if $-2A \leq -B - 2$.

The case $A \geq 1, B \geq 2$ was proved using our method in [1, Section 5]. This also implies the result for the symmetric case $A \leq -1, B \geq 2$. \square

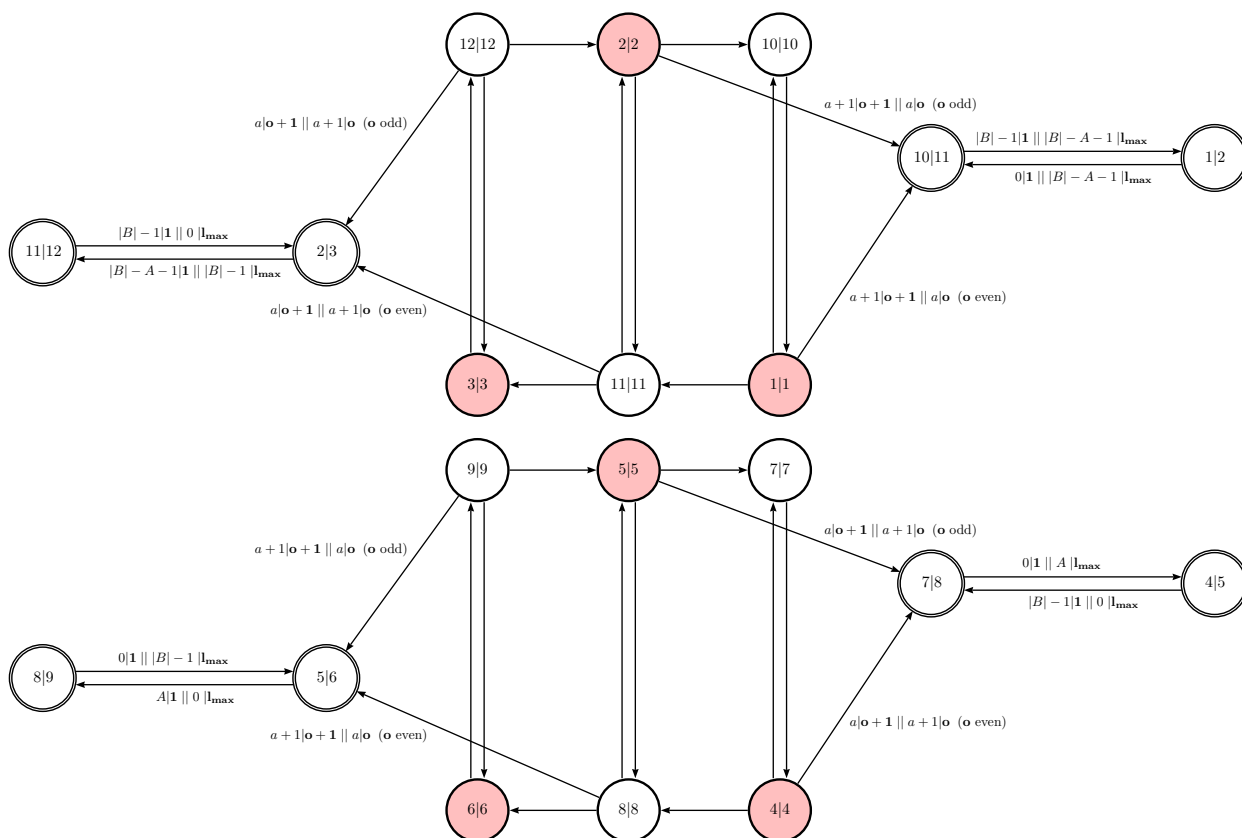


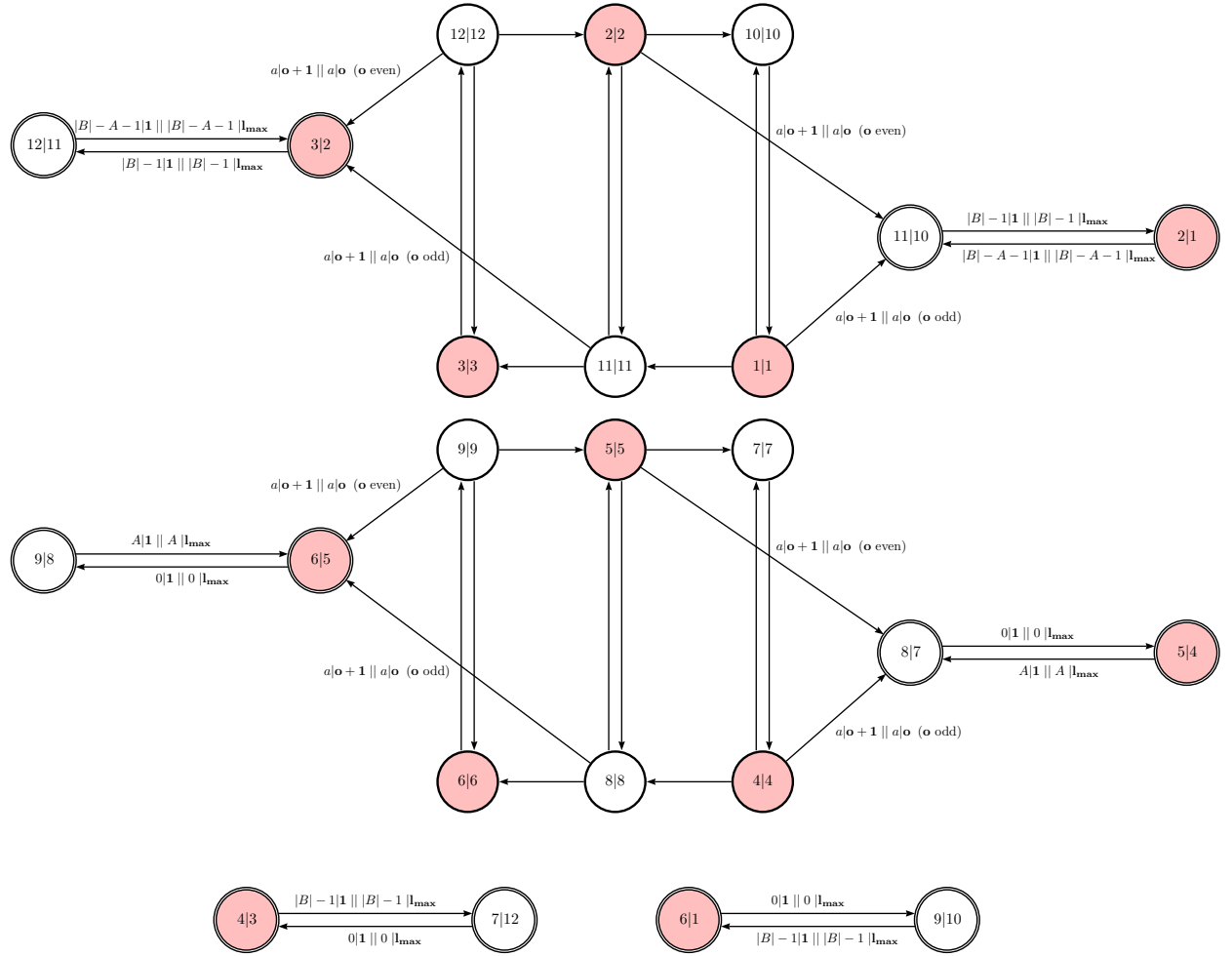
FIGURE 10. \mathcal{A}^ψ for $A \geq 1, B \leq -3$ and $2A \leq -B - 2$.

6. CONCLUDING REMARKS

In this paper, we gave an automatic proof of disk-likeness for a class of planar self-affine tiles with collinear digit set. It would be interesting to get further topological informations on the non-disk-like tiles. We expect this to be possible by use of our parametrization. The difficulty lies in the computation of the automaton giving the non trivial identifications, that is, the points where our parametrization fails to be injective. This is related to the complementation problem of Büchi automata. However in some applications, like the Heighway dragon, these identifications are “small” (for example countable) and the computations seem to be tractable (see forthcoming paper).

REFERENCES

- [1] S. AKIYAMA AND B. LORIDANT, *Boundary parametrization of self-affine tiles*, submitted.
- [2] S. AKIYAMA AND J. M. THUSWALDNER, *The topological structure of fractal tilings generated by quadratic number systems*, Computer And Mathematics With Applications, 49 (2005), pp. 1439–1485.
- [3] C. BANDT AND Y. WANG, Y., *Disk-like self-affine tiles in \mathbb{R}^2* , Discrete Comput. Geom. 26 (2001), no. 4, pp. 591–601.
- [4] F.M. DEKKING, *Replicating superfigures and endomorphisms of free groups*, J. Combin. Theory Ser. A 32 (1982), no. 3, pp. 315–320.
- [5] F.M. DEKKING, *Recurrent sets*, Adv. in Math. 44 (1982), no. 1, pp. 78–104.
- [6] J. M. DUMONT AND A. THOMAS *Systèmes de numération et fonctions fractales relatifs aux substitutions*, Theoret. Comput. Sci. 65 (1989), no. 2, pp. 153–169.
- [7] K. J. FALCONER, *Techniques in Fractal Geometry*, John Wiley and Sons, Chichester, New York, Weinheim, Brisbane, Singapore, Toronto, 1997.
- [8] K. GRÖCHENIG AND A. HAAS, *Self-similar lattice tilings*, J. Fourier Anal. Appl. 1 (1994), no. 2, pp. 131–170.

FIGURE 11. \mathcal{A}^{sl} for $A \geq 1, B \leq -3$ and $2A \leq -B - 2$.

- [9] X. G. HE AND K. S. LAU, *On a generalized dimension of self-affine fractals*, Math. Nachr. 281 (2008), no. 8, pp. 1142–1158.
- [10] J. E. HUTCHINSON, *Fractals and self-similarity*, Indiana Univ. Math. J., 30 (1981), no. 5, pp. 713–747.
- [11] K. H. INDLEKOFER, I. KATAI AND P. RACSKO, *Number systems and fractal geometry*, Probability theory and applications, Math. Appl., Kluwer Acad. Publ., Dordrecht, 80 (1992), pp. 319–334.
- [12] SH. ITO, *On the fractal curves induced from the complex radix expansion*, Tokyo J. Math. 12 (1989), no. 2, pp. 299–320.
- [13] I. KÁTAI, *Number systems and fractal geometry*, University of Pécs, 1995.
- [14] J. LAGARIAS AND Y. WANG, *Self-affine tiles in \mathbb{R}^n* , Adv. Math., 121 (1996), pp. 21–49.
- [15] J. LAGARIAS AND Y. WANG, *Integral self-affine tiles in \mathbb{R}^n . II. Lattice tilings*, J. Fourier Anal. Appl. 3 (1997), no. 1, pp. 83–102.
- [16] K.-S. LEUNG AND K.-S. LAU, *Disklikeness of planar self-affine tiles*, Trans. Amer. Math. Soc. 359 (2007), no. 7, pp. 3337–3355 (electronic).
- [17] J. LUO AND Y. M. YANG, *On single matrix graph directed iterated function systems*, preprint.
- [18] R. D. MAULDIN AND S. C. WILLIAMS, *Hausdorff dimension in graph directed constructions*, Trans. Amer. Math. Soc., 309 (1988), pp. 811–829.
- [19] K. SCHEICHER AND J. M. THUSWALDNER, *Canonical number systems, counting automata and fractals*, Math. Proc. Cambridge Philos. Soc., 133 (2002), pp. 163–182.
- [20] B. SOLOMYAK, *Dynamics of self-similar tilings*, Ergodic Theory Dynam. Systems 17 (1997), no. 3, pp. 695–738.
- [21] B. SOLOMYAK, *Tilings and dynamics*, Preprint, 51 pp., Lecture Notes, EMS Summer School on Combinatorics, Automata and Number Theory, 8-19 May 2006, Liege.

[22] H. J. SONG, *Replicating fractiles derived from digit systems in lattices*, unpublished.

DEPARTMENT OF MATHEMATICS, FACULTY OF SCIENCE, NIIGATA UNIVERSITY, IKARASHI 2 8050 NIIGATA, 950 2181, JAPAN

E-mail address: `akiyama@math.sc.niigata-u.ac.jp`

E-mail address: `loridant@math.sc.niigata-u.ac.jp`